Reaction Intermediate Analogues for Mandelate Racemase: Interaction between Asn 197 and the α-Hydroxyl of the Substrate Promotes Catalysis[†]

Martin St. Maurice and Stephen L. Bearne*

Department of Biochemistry and Molecular Biology, Dalhousie University, Halifax, Nova Scotia, B3H 4H7 Canada

Received May 19, 2000; Revised Manuscript Received August 15, 2000

ABSTRACT: Mandelate racemase (MR) catalyzes the interconversion of the enantiomers of mandelic acid, stabilizing the altered substrate in the transition state by 26 kcal/mol relative to the substrate in the ground state. To understand the origins of this binding discrimination, carboxylate-, phosphonate-, and hydroxamate-containing substrate and intermediate analogues were examined for their ability to inhibit MR. Comparison of the competitive inhibition constants revealed that an α-hydroxyl function is required for recognition of the ligand as an intermediate analogue. Two intermediate analogues, α-hydroxybenzylphosphonate (α-HBP) and benzohydroxamate, were bound with affinities approximately 100-fold greater than that observed for the substrate. Furthermore, MR bound α-HBP enantioselectively, displaying a 35-fold higher affinity for the (S)-enantiomer relative to the (R)-enantiomer. In the X-ray structure of mandelate racemase [Landro, J. A., Gerlt, J. A., Kozarich, J. W., Koo, C. W., Shah, V. J., Kenyon, G. L., Neidhart, D. J., Fujita, J., and Petsko, G. A. (1994) *Biochemistry 33*, 635−643], the α-hydroxyl function of the competitive inhibitor (S)-atrolactate is within hydrogen bonding distance of Asn 197. To demonstrate the importance of the α-hydroxyl function in intermediate binding, the N197A mutant was constructed. The values of k_{cat} for N197A were reduced 30-fold for (R)-mandelate and 179-fold for (S)-mandelate relative to wild-type MR; the values of k_{cat}/K_m were reduced 208-fold for (R)-mandelate and 556-fold for (S)-mandelate. N197A shows only a 3.5-fold reduction in its affinity for the substrate analogue (R)-atrolactate but a 51- and 18-fold reduction in affinity for α-HBP and benzohydroxamate, respectively. Thus, interaction between Asn 197 and the substrate's α-hydroxyl function provides approximately 3.5 kcal/mol of transition-state stabilization free energy to differentially stabilize the transition state relative to the ground state.

Mandelate racemase (E.C. 5.1.2.2) from *Pseudomonas putida* catalyzes the Mg^{2+}-dependent 1,1-proton transfer that interconverts the enantiomers of mandelic acid (Scheme 1) (*1−3*). This "pseudosymmetric" enzyme catalyzes the racemization of either substrate enantiomer with essentially identical kinetic parameters (*4*). Isotope exchange and site-directed mutagenesis experiments indicate that mandelic acid racemization proceeds by a two-base mechanism, with His 297 and Lys 166 abstracting the α-proton from (R)- and (S)-mandelate, respectively (*5−7*). In addition, site-directed mutagenesis experiments indicate that Glu 317 functions as a general acid catalyst (*8*). Mandelate racemase has been studied as a paradigm for enzymes that catalyze rapid carbon−hydrogen bond cleavage of carbon acids with relatively high pK_a values (*9−12*). To effect catalysis, mandelate racemase must overcome two problems. First, proton abstraction from carbon acids is inherently slow (*13−15*) so that the enzyme faces a kinetic barrier. Second, the enolate or enol intermediate formed is unstable (*16, 17*) and thus poses a thermodynamic problem for the enzyme.

Gerlt and Gassman have proposed that the high-energy intermediate formed during catalysis is an "enolic" species that is stabilized by formation of a strong "low-barrier" hydrogen bond to the γ-carboxyl function of Glu 317 (*8, 18−21*). Guthrie and Kluger (*22*) have argued that the problem is essentially thermodynamic and that electrostatic stabilization in combination with a reduction in medium polarity may be sufficient to stabilize the inherently unstable enol or enolate species formed during catalysis. Although the relative contributions of these two effects to catalysis are not known, it is clear that mandelate racemase is very proficient at discriminating between the substrate in the ground state and the altered substrate in the transition state, binding the latter species with an association constant equal to approximately 5×10^{18} M^{-1} and reducing the activation barrier for the reaction by 26 kcal/mol (*23*). One method of delineating the molecular origins of this discrimination is to examine the structures of enzymes complexed to substrates, products, and transition state or reactive intermediate analogues (*24*).

In the present work, we sought to develop reactive intermediate analogues as inhibitors of mandelate racemase. Enzymes, such as mandelate racemase, that are proficient at catalyzing the abstraction of a proton from the α-carbon of a carboxylic acid substrate are often strongly inhibited by analogues of the altered substrate in the transition state or of unstable intermediates that resemble the transition state (*25−30*). In these reactions, it is believed that the enzyme catalyzes carbon−hydrogen bond cleavage, in part, by
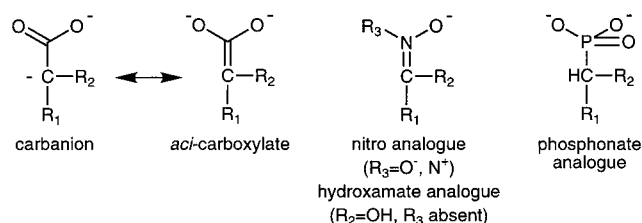
* To whom correspondence should be addressed. Phone: (902)494-1974; fax: (902)494-1355; e-mail: sbearne@is.dal.ca.

Scheme 1[a]
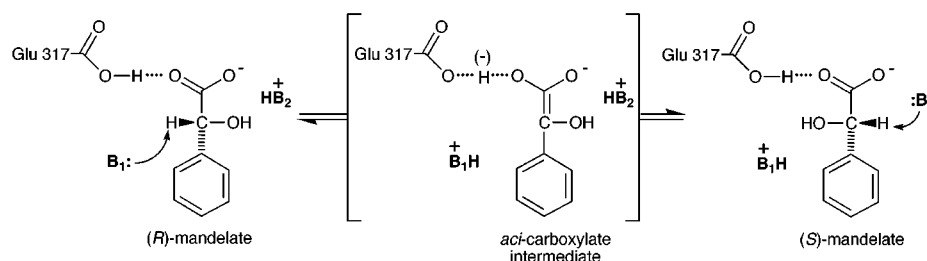
[a] **B**$_1$ and **B**$_2$ represent the active site bases His 297 and Lys 166, respectively.

Scheme 2

stabilizing the *aci*-carboxylate, a form of the carbanion with the negative charge delocalized into the carboxyl oxygens. Nitronate, hydroxamate, and phosphonate analogues of *aci*-carboxylate intermediates are potent inhibitors of a variety of enzymes catalyzing the formation of a carbanion α to a carboxyl group (Scheme 2). For example, nitro analogues of the substrates acted on by aspartase, fumarases (*31, 32*), aconitase (*33*), isocitrate lyase (*34*), enolase (*35, 36*), L-(+)-lactate dehydrogenase (*37*), adenoylsuccinate synthetase, and adenoylsuccinate lyase (*38, 39*) all inhibit these enzymes and are bound by the enzyme with an affinity much greater than that displayed for the analogous substrate. Both hydroxamate analogues (*35*) and phosphonate analogues (*40*) have been used to inhibit enolase, although the latter class of inhibitors only exhibited binding affinities similar to the substrate.

The present paper describes the competitive inhibition of mandelate racemase by carboxylate-, hydroxamate-, and phosphonate-containing analogues of the *aci*-carboxylate intermediate.[1] The α-hydroxyl function is identified as an important binding determinant for recognition of ligands as reactive intermediate analogues. α-Hydroxybenzylphosphonate (α-HBP)[2] and benzohydroxamate are identified as competitive inhibitors of mandelate racemase, binding to the enzyme more tightly than the substrate by 2 orders of magnitude. The carboxamide function of Asn 197 is hydrogen bonded to the α-hydroxyl function of ligands (*6, 8, 41−43*). Conversion of Asn 197 to an alanine residue by site-directed mutagenesis causes a 208- and 556-fold reduction

---

[1] Gerlt and Gassman (*20*) have used the term "enolic intermediate" to describe this species rather than terms such as "carbanion", "enolate" (*aci*-carboxylate), or "enol" (protonated *aci*-carboxylate) to avoid specifying the extent to which the proton is transferred from the active site general acidic catalyst (Glu 317) to the oxygen atom of the intermediate (Scheme 1). In agreement with Gerlt and Gassman, we do not mean to imply that the intermediate is an enolate, but we use the term *aci*-carboxylate to describe the structure of the intermediate in the enzyme-catalyzed reaction to facilitate comparison with the various analogues examined in the present work.

[2] Abbreviations: CD, circular dichroism; α-HBP, α-hydroxybenzylphosphonate; HEPES, 4-(2-hydroxyethyl)piperazine-1-ethanesulfonic acid; MES, 2-(*N*-morpholino)ethanesulfonic acid; TAPS, *N*-[tris-(hydroxymethyl)methyl]-3-aminopropanesulfonic acid.

in catalytic efficiency when either (*R*)- or (*S*)-mandelate is used as the substrate, respectively, indicating that the interaction between Asn 197 and the α-hydroxyl of mandelate stabilizes the altered substrate in the transition state by approximately 3.5 kcal/mol.

MATERIALS AND METHODS

Racemic, (*R*)-, and (*S*)-mandelic acid, benzohydroxamate, benzoylformate, phenylacetate, (1*S*,2*S*)-(−)-ephedrine, and (*S*)-(−)-α-methylbenzylamine were purchased from Sigma Chemical Company. AG 50W-X8 was purchased from BioRad. Benzylphosphonate was purchased from Lancaster Synthesis. Acetonitrile (HPLC-grade) was purchased from Fisher Scientific. All other reagents were purchased from Sigma Chemical Company. A clone of mandelate racemase from *Pseudomonas putida* in a pET-15b vector was obtained from Professor John Gerlt (University of Illinois). The pET-15b expression vector (Novagen) attaches a hexahistidine tag and a thrombin cleavage site to the N-terminus of the mandelate racemase polypeptide (MGSSHHHHHHSS-GLVPR ↓ GSHM$_1$ ... mandelate racemase). Plasmids containing the mandelate racemase gene were propagated in *Escherichia coli* strain DH5α cells and introduced into *E. coli* strain BL21(DE3) cells as the host for target gene expression. The enzyme was purified using metal ion affinity chromatography as described in the Novagen protocols (*44*). Synthetic oligonucleotide primers used for site-directed mutagenesis and DNA sequencing were purchased from ID Labs (London, Ontario). Standard techniques were used for DNA isolation, cloning, and both protein and DNA gel electrophoresis (*45*). NMR spectra were obtained using a Bruker AC 250F spectrometer. Chemical shifts (δ) for proton (^{1}H) and phosphorus (^{31}P) spectra are reported in ppm relative to 3-(trimethylsilyl)propanesulfonic acid and external H$_3$PO$_4$ (85% w/v in D$_2$O), respectively. Circular dichroism assays were conducted using a JASCO J-810 spectropolarimeter. Elemental analyses were conducted by Canadian Microanalytical Service Ltd. (Delta, BC).

α-*Hydroxybenzylphosphonate* (α-*HBP*). Dimethyl-(α-hydroxybenzyl)-[^{1}C]phosphonate [prepared by reaction of dimethyl phosphite with benzaldehyde as described by Abramov (*46*)] was demethylated by treatment with trimethylsilylbromide using a procedure similar to that described by Freeman et al. (*47*). Dimethyl-(α-hydroxybenzyl)-[^{1}C]phosphonate (0.5 g, 2.31 mmol) was dissolved in 5 mL of dry acetonitrile. Trimethylsilylbromide (1.5 mL, 11 mmol, 4.8 equiv) was added dropwise to the solution. The solution was refluxed for 30 min under an atmosphere of argon. Solvent was removed by rotary evaporation yielding a viscous yellow liquid. Dioxane (1.7 mL), water (1.7 mL), and cyclohexyl-

amine (0.8 mL) were added, and the solution was stirred for 40 min. After removal of the solvent by rotary evaporation, a white powder remained. This was dissolved in water (8.2 mL), and the solution was filtered. Acetone (74 mL) was added and a white precipitate, the cyclohexylamine salt, formed. The solution was stored at 4 °C for 1 h, and the precipitate was collected by suction filtration. The cyclohexylamine salt was then converted to the sodium salt by passing it through a AG 50W-X8 (Na$^+$ form) column. The eluent was collected, and the volume was reduced by rotary evaporation. Lyophilization yielded 0.267 g (55%) of a white powder: mp >300 °C; ^{1}H NMR δ (D$_2$O) 4.78 (1H, d, J_{P-H} 12.21, P$-$CH), 7.39 (5H, m); ^{31}P NMR δ (D$_2$O) 16.65 (s, ^{1}H decoupled; d, J_{P-H} 11.44, ^{1}H coupled). Anal. Calcd for C$_7$H$_7$O$_4$PNa$_2$: C, 36.22; H, 3.05; P, 13.34. Found: C, 36.36; H, 3.53; P, 13.34. The pK_a for ionization of the α-hydroxybenzylphosphonate monoanion (second pK_a) was determined to be 6.89 ± 0.01 by potentiometric titration (ionic strength maintained at 1.0 M using KCl; 23 °C).

Partial Resolution of (R)- and (S)-α-HBP. (R)- and (S)-α-HBP were partially resolved from a racemic mixture of the acid using a procedure similar to that described by Hoffmann (48). Racemic α-HBP (1.50 g, 8 mmol) and (1R,2S)-(−)-ephedrine hemihydrate (1.39 g, 8 mmol) were dissolved in 20 mL of boiling ethanol. The solution was cooled for 24 h at 4 °C. The precipitate (1.14 g) was collected using suction filtration, and 0.50 g of this precipitate was recrystallized from 95% ethanol. The salt was collected using suction filtration, dissolved in water, applied to a AG 50W-X8 (Na$^+$ form) column (2 × 40 cm), and eluted with water. Fractions containing the phosphonate were pooled and lyophilized to yield 0.13 g (39% yield) of the α-HBP sodium salt [α]$^{22}_D$ = +26.57° (c 0.2, H$_2$O). The specific rotation of this sample indicates that the (R)-α-HBP has been prepared with an enantiomeric excess equal to 76% [88% (R)-(+)-α-HBP and 12% (S)-(−)-α-HBP] based on the specific rotation of [α]$^{20}_D$ = +35° (c 1, H$_2$O) reported for enantiomerically pure (R)-(+)-α-HBP (48−50).

The filtrate from the preceding step was collected, applied to a AG 50W-X8 (H$^+$ form) column (2 × 40 cm), and eluted with water. Fractions containing the phosphonate were then pooled and lyophilized. The resulting phosphonic acid (0.39 g) was mixed with 0.25 g of (S)-(−)-α-methylbenzylamine and dissolved in 17 mL of boiling 90% ethanol. The solution was cooled at 4 °C for 48 h over which time an additional 10 mL of cold acetone was added. The resulting crystals were collected using suction filtration, dissolved in water, applied to a AG 50W-X8 (Na$^+$ form) column (2 × 40 cm), and eluted with water. Fractions containing the phosphonate were pooled and lyophilized to yield 35 mg (11% yield) of the α-HBP sodium salt [α]$^{22}_D$ = −28.66° (c 0.2, H$_2$O). The specific rotation of this sample indicates that the (S)-α-HBP has been prepared with an enantiomeric excess equal to 82% [91% (S)-(−)-α-HBP and 9% (R)-(+)-α-HBP].

Methyl α-Hydroxybenzylphosphonate. Sodium iodide (6.9 g, 46 mmol) and dimethyl (α-hydroxybenzyl)-[^{1}C]phosphonate (4.97 g, 23 mmol) were dissolved in dry acetone (150 mL). The solution was refluxed for 1 h and then cooled on ice producing a white precipitate. This precipitate was collected by suction filtration and dried under vacuum to yield a fine white powder (2.00 g, 39%): mp >300 °C; ^{1}H NMR δ (D$_2$O, ppm) 3.59 (3H, d, J_{P-H} 10.01, P$-$OCH$_3$), 4.91

(1H, d, J_{P-H} 12.21, P$-$CH), 7.41 (5H, m); ^{31}P NMR δ (D$_2$O) 19.89 (s, ^{1}H decoupled), 19.89 (m, ^{1}H coupled). Anal. Calcd for C$_8$H$_{10}$O$_4$PNa: C, 42.87; H, 4.51; P, 13.82. Found: C, 41.41; H, 4.41; P, 12.59.

Benzoylphosphonate. Dimethylbenzoylphosphonate was prepared by reaction of trimethyl phosphite with benzoyl chloride as described by Kluger and Chin (51). Dimethylbenzoylphosphonate was then demethylated by treatment with trimethylsilylbromide using the procedure of Sekine et al. (52) similar to that described for α-hydroxybenzylphosphonate. Bis(trimethylsilyl)benzoylphosphonate (3.37 g, 9.3 mmol) was treated with cyclohexylamine (2.3 mL, 20.4 mmol) to give the cyclohexylammonium salt (3.38 g, 95%) as described for the synthesis of α-hydroxybenzylphosphonate. The cyclohexylammonium salt was recrystallized from 95% ethanol and converted to the sodium salt by passing it through a AG 50W-X8 (Na$^+$ form) column. The eluent containing phosphonate was collected, and the volume was reduced by rotary evaporation. Lyophilization yielded a pale yellow powder: mp >300 °C; ^{1}H NMR δ (D$_2$O, ppm) 7.45 (phenyl H, m); ^{31}P NMR δ (D$_2$O) 0.37 (s, ^{1}H decoupled). Anal. Calcd for C$_7$H$_5$O$_4$PNa$_2$: C, 36.54; H, 2.19; P, 13.46. Found: C, 36.03; H, 2.29; P, 13.29.

Site-Directed Mutagenesis. The pET-15b plasmid containing the recombinant mandelate racemase gene was used as the template for polymerase chain reaction-based site-directed mutagenesis (QuickChange Site-Directed Mutagenesis Kit, Stratagene). The procedure followed was that described by the manufacturer. The two synthetic primers used to construct the N197A mutant were 5′-dGGCATCATGGTCGAC-TACGCCCAGAGTTTGGATGTACC-3′ and 5′-dGGTA-CATCCAAACTCTGGGCGTAGTCGACCATGATGCC-3′, where the positions of the mismatches are indicated by the underlined bases. The entire mutant gene was sequenced to verify that no other alterations in the nucleotide sequence had been introduced. The mutant enzyme, bearing a histidine tag, was purified using the same procedure as described for the wild-type enzyme. To verify that the conversion of Asn 197 to alanine did not cause any gross structural perturbations, the secondary structure was examined using CD spectroscopy. The CD spectra were recorded for both the histidine-tagged wild-type and the histidine-tagged mutant enzymes over a range from 182 to 260 nm in 10 mM sodium phosphate buffer, pH 7.5, and were analyzed for percent α-helix and β-sheet structure using CDNN CD Spectra Deconvolution v. 2.1 developed by G. Böhm. In addition, the K_m value for Mg^{2+} was determined for both wild-type and mutant enzymes using the method described by Fee et al. (53). Enzyme, freed of Mg^{2+}, was first incubated with the desired concentration of MgCl$_2$ for 5 (wild-type) or 10 min (N197A), and then the reaction was initiated by addition of (R)-mandelate (final concentration = 10 mM).

Mandelate Racemase Assays. Mandelate racemase activity was assayed using either the HPLC-based assay described previously by Bearne et al. (54) or the circular dichroism (CD) assay described by Sharp et al. (55). The HPLC assay was used to determine the inhibition constants for all of the intermediate analogues initially screened. Inhibition assays containing either α-HBP (9.5, 19.0, and 28.5 μM), methyl α-HBP (1.43, 2.85, and 5.70 mM), benzoylphosphonate (0.48, 0.95, and 1.90 mM), benzylphosphonate (2.38, 4.75, and 9.50 mM), benzohydroxamate (9.5, 19.0, and 28.5 μM),

phenylacetate (0.48, 0.95, and 1.90 mM), or benzoylformate (0.48, 0.95, and 1.90 mM) at the three concentrations indicated were conducted at 25 °C in 0.1 M Tris-HCl buffer, pH 7.5, containing 3.3 mM $MgCl_2$ and 15 ng/mL wild-type mandelate racemase. Substrate ((R)-mandelate) concentrations were 0.095, 0.238, 0.475, 0.950, 2.38, and 4.75 mM.

Inhibition of wild-type mandelate racemase activity by partially resolved (R)- and (S)-α-HBP was assayed in both the R→S and S→R directions using the CD assay. Assays were conducted at 25 °C in 0.1 M Na^+−HEPES buffer, pH 7.5, containing 3.3 mM $MgCl_2$. The substrate concentrations ((R)- or (S)-mandelate) were 0.238, 0.475, 0.95, 2.38, and 4.75 mM; the reactions were initiated by the addition of enzyme (final concentration = 100 ng/mL). The pH dependence of the kinetic parameters K_m and k_{cat} and the inhibition constant (K_i) for both α-HBP and benzohydroxamate were also determined using the CD assay. The enzyme was assayed using (R)-mandelate as a substrate in 0.1 M buffers containing 3.3 mM $MgCl_2$. The buffers used were 0.1 M MES, pH 6.3 and 6.7; 0.1 M HEPES, pH 6.7, 7.1, 7.5, and 7.9; and 0.1 M TAPS, pH 7.9, 8.3, 8.7, and 9.1. Initial velocities were determined using 100 ng/mL mandelate racemase with substrate concentrations of 0.238, 0.475, 0.950, 2.38, and 4.75 mM at each of three separate concentrations of inhibitor typically ranging between 0.95 and 475 μM for α-HBP and between 0.95 and 95 μM for benzohydroxamate depending on the pH of the assay.

The values of the kinetic parameters for the N197A mutant with respect to (R)-mandelate, (S)-mandelate, and Mg^{2+} were determined using the CD assay. Inhibition of the mutant's racemase activity by (R)-atrolactate, (R,S)-α-HBP, and benzohydroxamate was examined using the CD assay as described for the wild-type enzyme except that the mutant enzyme concentration in the assay ranged between 2 and 10 μg/mL.

In all assays, recombinant mandelate racemase bearing an N-terminal polyhistidine tag was used. Removal of this tag from the wild-type enzyme using thrombin-catalyzed cleavage (44) had no effect on k_{cat}, K_m, or enzyme inhibition by α-HBP. Kinetic data were analyzed by nonlinear regression analysis of Michaelis−Menten plots using the program EnzymeKinetics (Trinity Software, Compton, NH). Inhibition constants were determined in triplicate, and average values are reported. The reported errors are standard deviations. Protein concentrations were determined using the Bio-Rad Protein Assay (Bio-Rad Laboratories, Hercules, CA) with bovine serum albumin standards.

Deuterium Exchange Experiment. Wild-type mandelate racemase (440 ng/mL) was incubated either with 10 mM (R)-[α-¹H]mandelate or 10 mM (R,S)-[α-¹H]hydroxybenzylphosphonate for 1−12 h at 25 °C in 100 mM deuterated Tris-DCl buffer, pD 7.5, containing 3.3 mM $MgCl_2$. At various times, the reaction was terminated by boiling for 3 min. The samples were adjusted to pH 5 using 1 M HCl and passed through a AG 50W-X8 (Na^+ form) column (1.5 × 15 cm) to remove the buffer components. Eluent containing either mandelate or phosphonate was lyophilized and reconstituted in 600 μL of D_2O. Concentrated DCl (5 μL) was added to each sample to adjust the pD to ~1, and proton NMR was used to measure the peak area corresponding to the α-proton relative to the peak area corresponding to the phenyl protons (multiplet between 7.35 and 7.52 ppm).
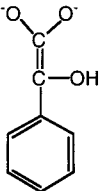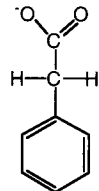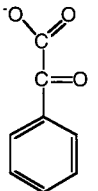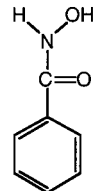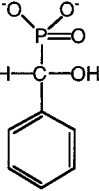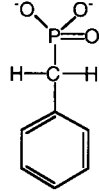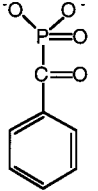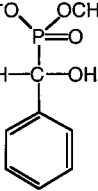
Relative peak areas were then used to calculate the percentage of deuterium incorporated at the α-position at various time points. Acidification of the sample was necessary to shift the signal corresponding to the α-proton of either mandelate (singlet at 5.01 ppm) or the phosphonate (doublet at 5.06 ppm) downfield from the HOD signal (4.82 ppm), thereby permitting accurate integration of the peak corresponding to the α-proton.

Molecular Electrostatic Potential Surfaces. Geometry optimizations and electrostatic potential surfaces were calculated for (R)-mandelate, benzoylformate, the putative *aci*-carboxylate intermediate, the (S)-α-hydroxybenzylphosphonate monoanion, and the conjugate base of *trans*-benzohydroxamate (O-deprotonated) by performing self-consistent-field calculations at the 6-31G* level using MacSpartan Plus (Wavefunction, Inc., Irvine, CA). Geometry optimizations and electrostatic potential surfaces for benzoylformate were calculated with free rotation of the carboxylate group restricted so that the carboxylate function was coplanar with the carbonyl group. This was done so that the resulting planar geometry was in agreement with that predicted using the semiempirical AM1 method contained within the MacSpartan Plus software.

RESULTS AND DISCUSSION

Mandelate racemase is a remarkably proficient enzyme, reducing the activation barrier for proton abstraction by 26 kcal/mol and producing a rate enhancement exceeding 15 orders of magnitude (23). Such proficient enzymes are expected to be extremely sensitive to inhibition by analogues of either transition states or high-energy intermediates formed during catalysis (25−30). Mandelate racemase catalyzes the interconversion of the two enantiomers of mandelic acid in a stepwise manner, with the abstraction of the α-proton from either enantiomer leading to the formation of an enolic/ate intermediate (56, 57). Gerlt and Gassman have proposed that concerted general acid−general base catalysis promotes both the enolization of the mandelate anion and ketonization of the enolic/ate intermediate (18−21). Guthrie and Kluger (22), on the other hand, have argued that the principal source of catalysis is electrostatic stabilization. Substrate and solvent deuterium isotope effect experiments conducted using the mutant enzymes H297N (7), E317Q (8), and K166R (42) further suggest that the reaction is stepwise. Although the precise structure of the transition state for the enolization reaction catalyzed by mandelate racemase is not known, it is reasonable to propose that it resembles either the putative *aci*-carboxylate intermediate or one of its conjugate acids.[1] Indeed, studies conducted on the nonenzymatic exchange of deuterium into the α-position of mandelate, a reaction that is mechanically similar to the enzyme-catalyzed reaction, support this proposal. The free energy of the transition state for the nonenzymatic exchange reaction has been estimated to be approximately 35 kcal/mol higher than the mandelate anion (23), while the neutral enol, enolate anion, and enolate dianion (*aci*-carboxylate) of mandelate lie 26.5, 25.3, and ~29 kcal/mol above mandelate at pH 7.5, 25 °C, respectively (23, 58, 59). Therefore, the structure of the transition state of the nonenzymatic exchange reaction is expected to resemble either the *aci*-carboxylate or one of its conjugate acids since these species have similar energies (59, 60).

Table 1: Competitive Inhibition of Mandelate Racemase by Carboxylate, Phosphonate, and Hydroxamate Analogues[a]

aci-carboxylate intermediate	Substrate Analogues		Intermediate Analogue
	phenylacetate $2.0\ (\pm 1.1) \times 10^{-4}$ M	benzoylformate $6.5\ (\pm 0.2) \times 10^{-4}$ M	benzohydroxamic acid $9.3\ (\pm 2.5) \times 10^{-6}$ M
Intermediate Analogues Containing the Phosphonate Function			
(R,S)-α-HBP $8.7\ (\pm 1.7) \times 10^{-6}$ M	benzylphosphonate[b] $3.5\ (\pm 1.3) \times 10^{-3}$ M	benzoylphosphonate $3.0\ (\pm 0.6) \times 10^{-4}$ M	(R,S)-methyl α-HBP $5.1\ (\pm 1.1) \times 10^{-3}$ M

[a] K_i values were determined using the HPLC assay and are shown under each compound. [b] Benzylphosphonate was incompatible with the HPLC column at high concentrations, and only a single K_i determination was performed. The reported error is the error in the regression line for the replot of K_m/V_{max} vs benzylphosphonate concentration. Re-determination of the inhibition constant using the CD assay gave a similar K_i value equal to $3.6\ (\pm 0.7) \times 10^{-3}$ M (average of three determinations).

To better understand the protein−ligand interactions that contribute to the stabilization of the altered substrate in the transition state at the active site of mandelate racemase, we sought to design transition state or reactive intermediate analogue inhibitors based on the structural and electronic characteristics of the *aci*-carboxylate intermediate. Since the substrate, the *aci*-carboxylate intermediate, and the product have very similar structures, there are only a limited number of structural changes that one can make that will mimic the electronic features of the intermediate while remaining approximately isosteric with the intermediate. Table 1 shows the structures of a number of such analogues. Each of these compounds was found to be a competitive inhibitor of mandelate racemase with respect to (R)-mandelate at pH 7.5. Of the seven analogues shown in Table 1, several bind with an affinity that is similar to that observed for the substrate, while others bind 2 orders of magnitude more tightly.

Inhibition by Carboxylate-Containing Analogues. Both phenylacetate and benzoylformate are bound to mandelate racemase with an affinity similar to that observed for binding of the substrate [$K_m = 0.79$ and 0.74 mM for (R)- and (S)-mandelate, respectively (*54*)[3]]. Phenylacetate, in which the α-hydroxyl group of mandelate is replaced by a hydrogen atom, appears to be bound by the enzyme only slightly better than the substrate. Benzoylformate has an sp^2 center at the α-carbon and, therefore, might be expected to mimic the *aci*-carboxylate intermediate. However, the enzyme's affinity for benzoylformate is almost identical to its affinity for the substrate. Thus, the presence or absence of a hydroxyl function on the α-carbon does not seem to affect binding of

the carboxylate-containing analogues. Mandelate racemase does not catalyze the exchange of the α-protons of phenylacetate with deuterated solvent despite having a similar affinity for both phenylacetate and mandelate (*41*), indicating that the α-hydroxyl function is required for catalysis. Indeed, crystal structures of wild-type mandelate racemase complexed with (R,S)-*p*-iodomandelate (*6*), α-phenylglycidate, or (S)-atrolactate (*41*) and mutant forms of mandelate racemase complexed with (S)-mandelate (*42*) or (S)-atrolactate (*8, 43*) all show the α-hydroxyl function coordinated to a magnesium ion, which is essential for catalysis (*53, 61*). Because coordination of the magnesium ion by the α-hydroxyl function appears to be important for stabilization of the altered substrate in the transition state (i.e., catalysis) and not substrate binding, one might expect the binding affinity of a transition state or reactive intermediate analogue to be extremely sensitive to the presence of a hydroxyl function at the α-position.

Inhibition by Phosphonate-Containing Analogues. The dianionic phosphonate function is expected to resemble the *aci*-carboxylate group of the putative intermediate (Scheme 2). Of the four phosphonate compounds examined as potential inhibitors of mandelate racemase, only α-hydroxybenzylphosphonate (α-HBP) was a potent inhibitor of the enzyme. Unlike the carboxylate-containing analogues, inhibition of mandelate racemase by the phosphonate analogues was greatly enhanced by the presence of a hydroxyl group on the α-carbon. Benzylphosphonate, in which the α-hydroxy group of α-HBP is replaced by a hydrogen atom, is bound by the enzyme approximately 400 times less tightly than α-HBP. The presence of a carbonyl group at the α-carbon position also reduces the binding affinity as evidenced by the 100-fold increase in the K_i value for benzoylphosphonate relative to α-HBP. It is unlikely that this weak binding,

---

[3] Both (R)- and (S)-mandelate protect mandelate racemase from inactivation by (R,S)-α-phenylglycidate. The dissociation constant for the substrate in the protection experiments (K_S) agrees well with the value of K_m (*61*). Thus, for mandelate racemase, $K_m \approx K_S$.
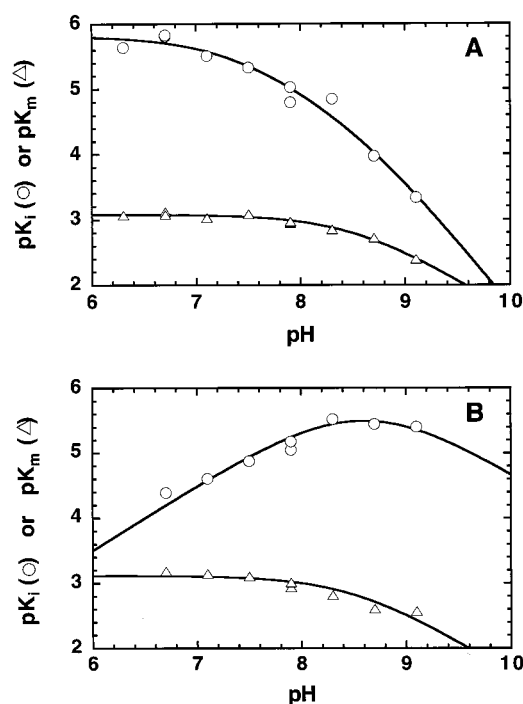
FIGURE 1: pH dependence of pK_i (○) and pK_m (△) for the competitive inhibition of mandelate racemase by α-HBP (A) and benzohydroxamate (B) with respect to (R)-mandelate. Assay conditions are as described in Materials and Methods. The curves shown for the pK_m data in both panels A and B were based on the assumption that a single ionization in the free enzyme occurred over the pH range studied and fit to the equation $pK_m = p\tilde{K}_m - \log(10^{-pH} + 10^{-pK_a^e})$, where K_m is the apparent Michaelis constant, $\tilde{K}_m$ is the pH-independent Michaelis constant, and K_a^e represents the ionization constant for the free enzyme. The curve shown for the pK_i data in panel A was fit to the equation $pK_i = p\tilde{K}_i - \log(10^{-pH} + 10^{-pK_a^i}) - \log(10^{-pH} + 10^{-pK_a^e}) - 2\,pH$, where K_i is the apparent inhibition constant, $\tilde{K}_i$ is the pH-independent inhibition constant, K_a^i represents the ionization constant for the free inhibitor, and K_a^e represents the ionization constant for the free enzyme. This equation describes a single ionization in both the free enzyme and the free inhibitor, where the inhibitor is bound exclusively in the *protonated* ionization state (Scheme 3A). The value of pK_a^i for α-HBP was 7.3 ± 0.3 using a pK_a^e value of 8.52 ± 0.04 (obtained from the fit of the corresponding pK_m data). The curve shown for the pK_i data in panel B was fit to the equation $pK_i = p\tilde{K}_i - pK_a - \log(10^{-pH} + 10^{-pK_a^i}) - \log(10^{-pH} + 10^{-pK_a^e}) - pH$. This equation describes a single ionization in both the free enzyme and the free inhibitor where the inhibitor is bound exclusively in the *unprotonated* ionization state (Scheme 3B). The value of pK_a^i for benzohydroxamate was 8.7 ± 0.3, using a pK_a^e value of 8.51 ± 0.13 (obtained from a fit of the corresponding pK_m data).

relative to the α-hydroxylated phosphonate, arises due to a difference between each compound's ability to chelate the active site magnesium ion. Comparison of the stability constants for the chelation of divalent metal ions (Zn^{2+} and Cu^{2+}) by α-ketobutyric acid as compared to 2-hydroxybutanoic acid and by acetoacetate as compared to 3-hydroxybutyric acid (62) indicates that, while α-hydroxy acids tend to form slightly stronger chelates than the corresponding keto acids by factors ranging between 1.1 and 3.2, this added strength of association with the metal ion is certainly not enough to account for the observed 100-fold decrease in binding affinity. A more likely explanation for the weak binding is that the functional group on the α-carbon must be a hydrogen bond donor. Thus it appears that mandelate

Scheme 3[a]

A.

B.
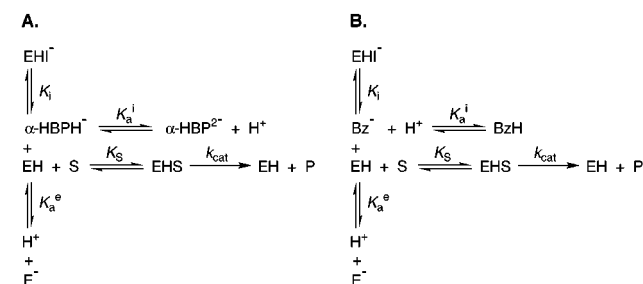
[a] Kinetic mechanisms describing the observed pH dependence of inhibition by α-HBP (A) and benzohydroxyamate (B).

racemase is sensitive to the presence of the hydroxyl function at the α-position of the phosphonate analogues. Therefore, α-HBP may be regarded as a mimic of the *aci*-carboxylate intermediate or of the transition states for the intermediate's formation starting from either substrate enantiomer (60).

The pH dependence of the inhibition of mandelate racemase by α-HBP was investigated to determine which ionization state of the phosphonate function is preferentially bound by the enzyme. Figure 1A shows that as the pH was increased from 6.3 to 9.1; the observed pK_i value for α-HBP decreased to a limiting slope of -2 with respect to pH. This is consistent with two ionizations contributing to the observed loss of inhibition at higher pH values (Scheme 3A) (63, 64). On the other hand, the observed pK_m value for (R)-mandelate remained unchanged over pH values ranging between 6.3 and 8.3 and then decreased above pH 8.5 approaching a limiting slope of -1 with respect to pH. This downward curvature in the pK_m vs pH plot is consistent with a single ionization occurring on the free enzyme (63, 64). Using these data, the pK_a^i and pK_a^e values for the ionization of the phosphonate function on α-HBP and a group on the free enzyme were determined to be 7.3 ± 0.3 and 8.5 ± 0.1, respectively (Figure 1A). The observed value of pK_a^i agrees well with the value of 6.89 ± 0.01 determined potentiometrically (data not shown) for the pK_a of the α-HBP monoanion. Thus, optimal inhibition by α-HBP is observed when the free enzyme is protonated and the phosphonate function of α-HBP is monoanionic.

It is not clear why the enzyme preferentially binds the monoanionic species. The most likely explanation is that residues in the active site are arranged to optimally bind the planar carboxylate or *aci*-carboxylate function and not a phosphonate function in which the negatively charged oxygen atoms are tetrahedrally arranged about the phosphorus atom. The two oxygens sharing the formal negative charge on the phosphonate monoanion, however, could mimic the planar carboxylate or *aci*-carboxylate function while the remaining phosphonate oxygen is protonated (discussed below).[4]

---

[4] Since it is possible that the intermediate might have enolic character, one might expect the monoanionic phosphonate function to mimic the protonated *aci*-carboxylate. However, this places the partially delocalized negative charge of the monoanion above the plane defined by the HO−P−O⁻ bonds, a configuration which resembles that expected for the phosphonate dianion (Scheme 4) and appears to be unfavorable (see Discussion). In addition, if the developing negative charge on the carbonyl oxygen is one of the features that permits the active site to stabilize the intermediate through proton transfer from the general acidic catalyst (8, 12), then one would expect proton transfer to the anionic oxygen of a phosphonate to be a significant factor in analogue binding.
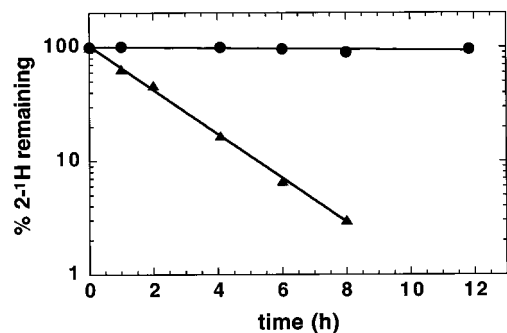
FIGURE 2: Time dependence for the exchange of the α-proton of (*R*)-mandelate (▲) and (*R*,*S*)-α-HBP (●) with solvent (D₂O) catalyzed by mandelate racemase. The proton NMR signals were integrated after incubation of 10 mM (*R*)-[α-¹H]mandelate or 10 mM (*R*,*S*)-[α-¹H]hydroxybenzylphosphonate with 440 ng/mL mandelate racemase for the indicated reaction times. Reaction conditions are as described in Materials and Methods. The peak area corresponding to the signal of the α-proton of either (*R*)-[α-¹H]-mandelate or (*R*,*S*)-[α-¹H]hydroxybenzylphosphonate was measured relative to the peak area of the signal corresponding to the protons of the phenyl ring at the indicated times.

Deuterium exchange experiments were conducted to determine whether α-HBP could act as a substrate for mandelate racemase (Figure 2). Proton NMR was used to follow the exchange of deuterium from solvent (D₂O) into the α-position of both mandelate and (*R*,*S*)-[α-¹H]HBP. While mandelate completely exchanged its α-proton in a first-order process, α-HBP did not exchange its α-proton with solvent over 24 h, indicating that it was not a substrate in the reaction catalyzed by mandelate racemase. It is unlikely that differences in the electron-withdrawing abilities of the phosphonate and carboxylate functions account for this observed lack of reactivity. The monoanionic phosphonate function is only slightly more electron withdrawing (σ_{para} = 0.17) than the carboxylate function, while the dianionic phosphonate function is slightly electron donating (σ_{para} = −0.16) (*65*). A more likely explanation is that the α-hydrogen atom is not correctly positioned for abstraction. The added steric bulk of the phosphonate function could alter the position and orientation of α-HBP in the active site relative to that normally occupied by mandelate. The importance of steric bulk is illustrated by the observation that mandelate racemase binds methyl α-HBP with much less affinity than it binds α-HBP. In addition to steric differences, the monoanionic phosphonate does not possess a rotationally symmetrical charge distribution like the carboxylate (discussed below). The consequence of this difference in angular charge distribution is that α-HBP may bind in a "skewed" orientation and therefore behave as an inhibitor and not a substrate of the enzyme (*40, 66*).

Enantioselective Binding of α-HBP. The inhibition of mandelate racemase by the individual enantiomers of α-HBP was investigated with respect to both (*R*)- and (*S*)-mandelate (Table 2). Both (*R*)- and (*S*)-α-HBP were fractionally crystallized to a high enantiomeric excess. Mandelate racemase bound (*S*)-α-HBP with an affinity that was 30−40-fold greater than that observed for (*R*)-α-HBP. This result provides the first example of an intermediate analogue which unmasks a "functional asymmetry" within the active site of mandelate racemase. While such a strong binding preference for one enantiomer over the other is unexpected for a "pseudosymmetric" enzyme such as mandelate racemase,

Table 2: Inhibition of Mandelate Racemase by Mixtures of the Enantiomers of α-Hydroxybenzylphosphonate[a]

mixture of α-HBP enantiomers	ee (%)	K_i (μM)	
		(*R*) → (*S*)	(*S*) → (*R*)
(*R*,*S*)	0	4.7 ± 0.7	3.9 ± 0.9
(*S*)	82	1.1 ± 0.3	1.6 ± 0.2
(*R*)	76	34 ± 9	35 ± 2

[a] K_i values were determined using the CD assay.

enantioselective binding preferences have been noted for the competitive inhibitors (*R*)- and (*S*)-atrolactate as well as for the irreversible inhibitor (*R*)-phenylglycidate (*41*). It is of interest to note that while both (*S*)-atrolactate and (*R*)-phenylglycidate have the same relative configuration of atoms about the α-carbon as (*S*)-mandelate, the configuration of atoms about the α-carbon of (*S*)-α-HBP resembles (*R*)-mandelate. The most likely explanation for the observed binding preference for (*S*)-α-HBP relative to (*R*)-α-HBP is that skewed binding induced by the phosphonate function and the resulting altered position of the α-hydroxyl function produces different interactions between active site residues and the two enantiomeric ligands.

Inhibition by Benzohydroxamate. Like α-HBP, benzohydroxamate is also a potent inhibitor of mandelate racemase, binding 2 orders of magnitude more tightly than the substrate. This result is interesting in light of the recent report that D-glucarate dehydratase, a member of the mandelate racemase subgroup of the enolase superfamily of enzymes, binds xylarohydroxamate with an affinity (K_i = 0.8 mM; K_m for D-glucarate = 0.16 mM) that is much lower than would be expected if the hydroxamate was a mimic of the enolic intermediate (*67*). The pH dependence of the inhibition was investigated to determine which ionization state of benzohydroxamate is preferentially bound by the enzyme (Figure 2B). As the pH was increased from 6.7 to 9.1, the observed pK_i value followed a roughly bell-shaped curve with limiting slopes of +1 and −1 with respect to pH. Again, the pK_m value for (*R*)-mandelate remained unchanged over pH values between 6.7 and 8.3 and then decreased above pH 8.3 approaching a limiting slope of −1 with respect to pH. Using these data, the pK_a^i and pK_a^e values for the ionization of benzohydroxamate and a group on the free enzyme were determined to be 8.7 ± 0.3 and 8.5 ± 0.1, respectively (Figure 2B and Scheme 3B). The pK_a^i value of 8.7 ± 0.3 is in excellent agreement with the pK_a value of 8.8 for benzohydroxamic acid (*68*). Thus, mandelate racemase preferentially binds the deprotonated form of benzohydroxamic acid.

Since benzohydroxamic acid possesses two sites of deprotonation, i.e., nitrogen and oxygen, several structures may exist in solution, and the actual structure of the conjugate base of benzohydroxamic acid has been the subject of a long-standing debate (*68−70*). In water, benzohydroxamic acid exists primarily in the keto form, and both of the conjugate bases arising from O- and N-deprotonation have been observed depending on the dielectric of the solvent. The O-deprotonated form of the enol has never been observed (*68*). In water, experimental evidence suggests that benzohydroxamate undergoes O-deprotonation (*68*), yielding a species that resembles benzoylformate more than the putative *aci*-carboxylate intermediate. If mandelate racemase recog-
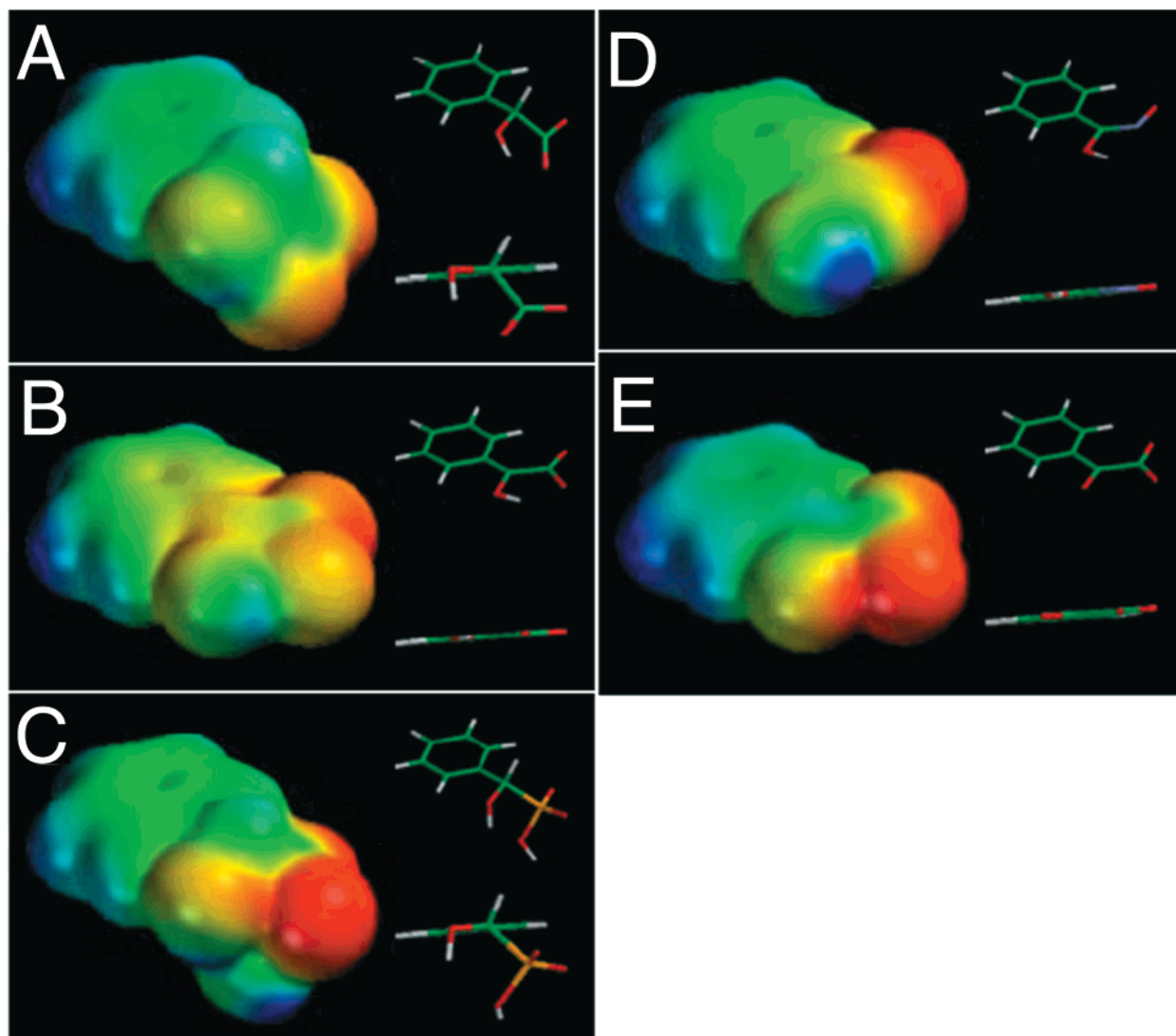
FIGURE 3: Molecular electrostatic potential surface at the van der Waals radii for (*R*)-mandelate (A), the putative *aci*-carboxylate intermediate (B), the (*S*)-α-hydroxybenzylphosphonate monoanion (C), the conjugate base of *trans*-benzohydroxamate (*O*-deprotonated) (D), and benzoylformate (E). Color-coded electrostatic potential surfaces are shown for each of these ligands with an electron density isosurface displayed at a density of 0.002 e/a$_0^3$, which encompasses approximately 95% of the van der Waals radii (*87*). The red regions are the most negative potentials, and the blue regions are the most positive on the electrostatic potential surfaces. The energy difference from the red to blue regions is approximately 131 kcal/mol. The stick models in the upper right corner of each panel have the same orientation as the electrostatic potential surface models while those in the lower right corner have been rotated to more clearly display the plane of the phenyl ring. The stick models use the colors red, blue, green, white, and yellow to represent oxygen, nitrogen, carbon, hydrogen, and phosphorus, respectively.

nizes the α-hydroxyl function as an important binding determinant of the reactive intermediate, as suggested by the carboxylate and phosphonate analogue studies, one would not expect the enzyme to bind benzohydroxamate with the observed high affinity. On the other hand, the O-deprotonated form of the benzohydroxamic acid enol (*cis* or *trans*) more closely resembles the putative *aci*-carboxylate intermediate. Mandelate racemase may stabilize this rare form of the inhibitor, promoting O-deprotonation of the enol to yield the monoanionic species within the active site.

Electrostatic Potential Surfaces and Stereoelectronic Effects. Enzymes effect chemistry by inducing changes in electron distribution in substrates (*71*). Generation of differential charge distribution between the substrate and the altered substrate in the transition state permits electrostatic interactions between the enzyme and its ligand to selectively stabilize the transition state (*72*). Elegant studies conducted

by Schramm and co-workers have focused on calculating the electrostatic potential surfaces of enzyme-bound transition-state structures deduced from kinetic isotope effects (*73*−*75*). These studies have revealed that as the structure of the substrate is altered to that of the transition state, there are changes in the electrostatic potential surface which an enzyme may utilize to selectively bind and stabilize the transition state relative to the ground state. Although the detailed geometric and electronic characteristics are not yet available for the mandelate racemase-bound transition state, we have calculated the electrostatic potential surfaces of the putative *aci*-carboxylate intermediate in the gas phase so that its electrostatic potential surface may be compared to the inhibitors described in the present work.

Geometry optimizations and electrostatic potential surfaces were calculated for (*R*)-mandelate, the putative *aci*-carboxylate intermediate, the (*S*)-α-HBP monoanion, the conjugate base

base of *trans*-benzohydroxamate (O-deprotonated) and benzoylformate by performing self-consistent field calculations at the 6-31G* level. The color-coded electrostatic potential surfaces for each of these ligands are displayed in Figure 3. It should be noted that the geometries of these species were optimized in the gas phase and are not intended to represent the conformation assumed by the bound ligand at the active site.

The electrostatic potential surface for (*R*)-mandelate (Figure 3A) indicates that the negative potential is primarily localized on the carboxylate function of the substrate. On the other hand, the *aci*-carboxylate intermediate (Figure 3B) has the negative charge delocalized over the entire molecule. The optimized geometry and calculated electrostatic potential surfaces for the conjugate base of (*S*)-α-HBP and *trans*-benzohydroxamate (O-deprotonated) are shown in Figure 3, panels C and D, respectively. Although the electrostatic potential surface of (*S*)-α-HBP appears to resemble aspects of both the substrate and the *aci*-carboxylate intermediate, the oxygen atoms of the phosphonate function may be oriented so that the negative charge is almost coplanar with the phenyl ring thereby mimicking the *aci*-carboxylate as indicated in the stick diagrams (Figure 3C). While several different forms of benzohydroxamate are theoretically possible, either the *cis*- or *trans*-benzohydroxamate (O-deprotonated) most closely resembles the *aci*-carboxylate intermediate (vide supra). The O-deprotonated *trans*-benzohydroxamate is planar and has an electrostatic potential surface that closely mimics the *aci*-carboxylate intermediate. The optimized geometry (with restrictions imposed on the rotation of carboxylate group) and calculated electrostatic potential surfaces for the carboxylate-containing analogue, benzoylformate, is shown in Figure 3E. Because of its sp²-hybridized α-carbon, benzoylformate has an electrostatic potential surface very similar to the planar *aci*-carboxylate intermediate. The fact that benzoylformate is a poor inhibitor of the enzyme emphasizes the important role that the α-hydroxyl function plays in the binding of intermediate analogues.

In addition to the electrostatic potential surfaces, stereoelectronic factors play a role in the orientation of phosphonate-containing ligands in an enzyme's active site (*40, 66*). During catalysis by mandelate racemase, it is reasonable to assume that the position of the carboxyl and α-hydroxyl groups on bound ligands remain relatively fixed in orientation within the active site. This would permit stabilization of the enolic/ate intermediate by hydrogen bonding with Glu 317 (*8*) and electrophilic catalysis through coordination to the magnesium ion (*6, 53*). Indeed, the crystal structures of both wild-type and mutant forms of mandelate racemase complexed to substrate or substrate analogues reveal that several amino acid side chains specifically interact with the carboxyl and α-hydroxyl groups, including Ser 139, Lys 164, Asn 197, Glu 317, and Glu 247 (*6*). Bearing this requirement in mind, a stereoelectronic feature of the ligands that must be considered is their angular charge distribution (Scheme 4). In the carboxylate of (*R*)-mandelate and the *aci*-carboxylate, the negative charge is rotationally symmetrical about the line which bisects the angle made by the carboxyl carbon and the two anionic oxygens. This line also makes an angle of 180° relative to the bond between the carboxyl carbon and the α-carbon. The negative charge of the α-HBP dianion is also rotationally symmetrical with respect to such a line.

Scheme 4[a]

(*R*)-mandelate

aci-carboxylate intermediate

α-HBP monoanion

α-HBP dianion

α-HBP monoanion
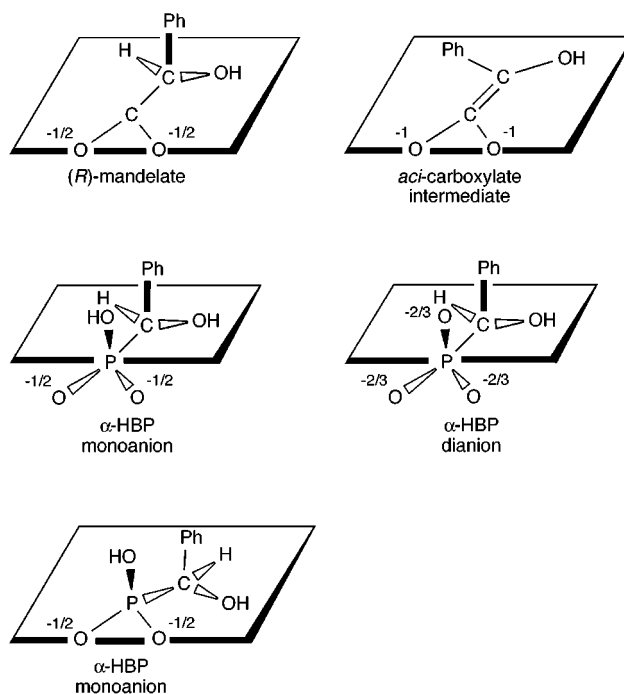
[a] α-HBP is shown binding in a "skewed" orientation when the phosphonate oxygens bearing the negative charge are located in the same plane as the oxygens of the *aci*-carboxylate intermediate. Solid and open wedges are used for groups that lie above and below the indicated planes.

However, this is not the case for the α-HBP monoanion. Orientation of monoanionic phosphonate function so that the vector of its negative charge aligns with that of the substrate or *aci*-carboxylate intermediate results in skewed binding of this analogue as illustrated in Scheme 4. As mentioned earlier, this may account for why the α-HBP monoanion is an inhibitor of mandelate racemase and not a substrate. In the absence of structural data, it is not clear why the phosphonate dianion is not preferentially bound at the active site of mandelate racemase. One explanation is that the enzyme cannot tolerate a negatively charged substituent above the plane defined by the carboxylate function as shown in Scheme 4.

Kinetics of the N197A Mutant. The sensitivity of mandelate racemase to the presence of an α-hydroxyl function on the phosphonate analogues prompted us to investigate the contribution of Asn 197 to catalysis. In all published crystal structures of wild-type and mutant forms of mandelate racemase, the carboxamide of this residue is within hydrogen-bonding distance of the α-hydroxyl function of bound ligands as shown in Figure 4 (*6, 8, 41−43*). The γ-carboxylate of Glu 247 is also within hydrogen-bonding distance of the α-hydroxyl group but is involved in coordinating the magnesium ion (*6*).

Site-directed mutagenesis was used to replace Asn 197 with alanine. The introduction of alanine did not significantly alter the secondary structure of the protein nor did it significantly perturb the K_m value for Mg^{2+} relative to the wild-type enzyme (Table 3). However, a marked effect on catalysis was observed. The value of k_{cat} was reduced 30- and 179-fold for catalysis in the $R \rightarrow S$ and $S \rightarrow R$ directions, respectively. Interestingly, the mutation had little effect on substrate binding with K_m increasing only 7- and 2-fold for

Table 3: Kinetic Parameters and Inhibition Constants for Wild-Type and N197A Mandelate Racemase[a]

parameter	wild-type	N197A	N197A/wild-type
% α content	38.9 (40.4)[b]	34.6	
% β content	25.5 (19.5)[b]	27.6	
$K_m (Mg^{2+})$, mM	0.65 ± 0.06	0.34 ± 0.08	
$k_{cat} (R) \rightarrow (S)$, s^{-1}	514 ± 48	16.9 ± 3.5	0.033 ± 0.007
$K_m ((R)$-mandelate), mM	0.81 ± 0.12	5.40 ± 0.66	6.67 ± 1.28
$k_{cat}/K_m (R) \rightarrow (S)$, $M^{-1} s^{-1}$	$6.4 (\pm 1.1) \times 10^5$	$3.1 (\pm 0.7) \times 10^3$	$4.8 (\pm 1.4) \times 10^{-3}$
$k_{cat} (S) \rightarrow (R)$, s^{-1}	447 ± 12	2.5 ± 0.6	$5.6 (\pm 1.4) \times 10^{-3}$
$K_m ((S)$-mandelate), mM	0.62 ± 0.04	1.40 ± 0.43	$2.25 (\pm 0.71)$
$k_{cat}/K_m (S) \rightarrow (R)$, $M^{-1} s^{-1 c}$	$7.2 (\pm 0.5) \times 10^5$	$1.3 (\pm 0.5) \times 10^3$	$1.8 (\pm 0.7) \times 10^{-3}$
$K_i ((R,S)$-α-HBP), mM	0.0047 ± 0.0007	0.238 ± 0.064	51 ± 16
K_i (benzohydroxamate), mM	0.0117 ± 0.0012	0.216 ± 0.006	18 ± 2
$K_i ((R)$-atrolactate), mM	0.95 ± 0.33	3.30 ± 0.33	3.5 ± 0.4

[a] Kinetic constants and K_i values were determined using the CD assay. [b] Secondary structure content reported for the X-ray crystal structure of wild-type mandelate racemase complexed with (S)-atrolactate (41) is shown in parentheses. Values determined in the present work are for the wild-type and N197A enzymes bearing the histidine tag. [c] For a racemase, the equilibrium constant (K_{eq}) for the reaction is unity. Thus for mandelate racemase, the Haldane relationship (88) requires that $(k_{cat}/K_m)^{(R)\rightarrow(S)}/(k_{cat}/K_m)^{(S)\rightarrow(R)} = K_{eq} = 1$. For wild-type mandelate racemase, $K_{eq} = 0.9$ (± 0.2); however, for N197A, $K_{eq} = 2.4$ (± 1.1). The large error in K_{eq} for N197A reflects the difficulty in measuring the kinetic parameters where K_m is increased and k_{cat} is markedly reduced relative to the wild-type enzyme.
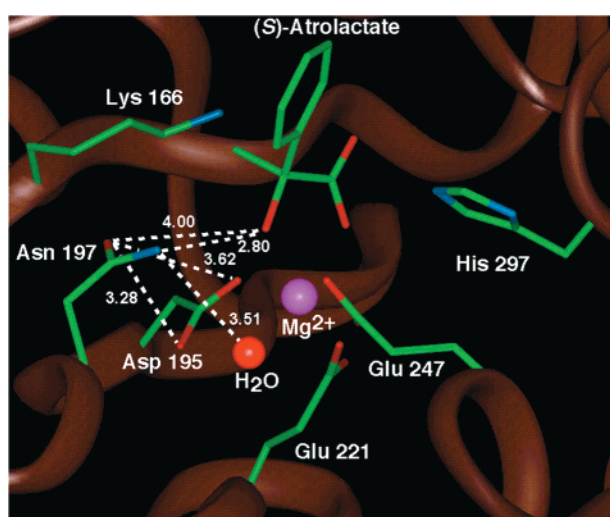

FIGURE 4: X-ray crystal structure of the active site of wild-type mandelate racemase with bound (S)-atrolactate (MDL; 41). The catalytic bases (Lys 166 and His 297) and residues coordinating the magnesium ion (Asp 195, Glu 221, Glu 247, and water) are shown. Asn 197 and the distances (Å) between the carboxamide function and (S)-atrolactate, Asp 195, and the water molecule are also shown. The assignment of the position of the C=O and −NH₂ within the plane of the carboxamide of Asn 197 is completely arbitrary at the resolution of the crystal structure (Gregory A. Petsko, personal communication). Oxygen, nitrogen, and carbon atoms are red, blue, and green, respectively. The α-carbon backbone is brown.

FIGURE 5: Free energy profile (pH 7.5, 25 °C) for the racemization of (R)-mandelate ((**R**)) and (S)-mandelate ((**S**)) by wild-type and N197A mandelate racemases. The profiles are derived from the kinetic parameters in Table 3. ES‡ represents the enzyme−substrate complex in the transition state.

(R)- and (S)-mandelate, respectively. Thus, interaction of Asn 197 with the α-hydroxyl of the substrate stabilizes the altered substrate in the transition state by 3.2−3.7 kcal/mol. This agrees well with the additional 3.5 kcal/mol that the α-hydroxyl contributes to the binding of α-HBP relative to benzylphosphonate.

The transition state stabilization provided by the interaction between Asn 197 and the α-hydroxyl function of mandelate fits into the range of values expected for residues participating in neutral hydrogen bond pairs (64, 76−78). For example, Roth et al. (79) have reported that His 357 of *E. coli* β-galactosidase interacts with the C3 hydroxyl of the ligand and stabilizes the transition state by approximately 3.5 kcal/mol. Since Asn 197 stabilizes the altered substrate in the transition state more than it stabilizes the substrate in the ground state [differential binding (80, 81)], the binding
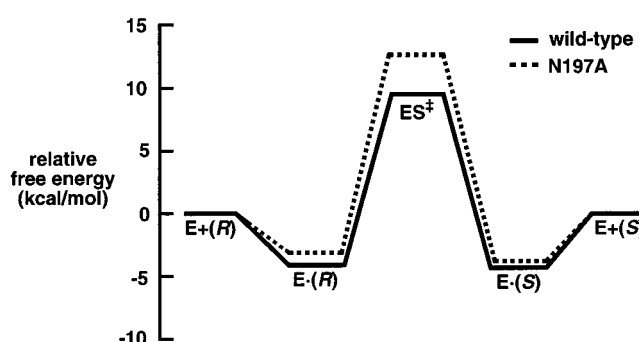
affinity of intermediate analogue inhibitors to the N197A mutant would be expected to be reduced relative to the wild-type enzyme while the binding affinity of ground state analogues would not be significantly affected. Indeed, binding of both α-HBP and benzohydroxamate by the N197A mutant is much more severely affected than is the binding of (R)-mandelate, (S)-mandelate, or (R)-atrolactate (Table 3). The free energy profiles for racemization catalyzed by both the wild-type and N197A racemases, shown in Figure 5, illustrate how the interaction between Asn 197 and the α-hydroxyl results in preferential binding of the altered substrate in the transition state relative to the ground state.

What is the structural basis for Asn 197's apparent discrimination between the substrate in the ground state and the altered substrate in the transition state? Figure 4 reveals that the carboxamide of Asn 197 lies within hydrogen bonding distance of the ligand's α-hydroxyl function. The weak inhibition observed for benzoylformate and benzoylphosphonate in the present study indicates that the enzyme displays a higher affinity for ligands with a hydrogen bond donor at the α-position.[5] Therefore, it is likely that the

[5] Preliminary studies in our laboratory using the competitive inhibitor (R,S)-α-fluorobenzylphosphonate indicate that mandelate racemase has a weak affinity ($K_i = 0.25 \pm 0.06$ mM) for this compound (St. Maurice, Bearne, and Taylor, unpublished observations). This finding supports the notion that potent inhibition occurs when a hydrogen bond donor is present at the α-position rather than a hydrogen bond acceptor.

carboxamide oxygen of Asn 197 acts as the hydrogen bond acceptor (i.e., the carboxamide function is rotated 180° from the orientation shown in Figure 4).

As the intermediate is formed, the pK_a of the α-hydroxyl would be expected to decrease as the oxygen becomes enolic in the intermediate. For example, the pK_a of 2-propanol is 18 (*82*) while pK_a of enolic acetone is 10.9 (*83*). However, it is unlikely that these alterations in pK_a values are sufficient to account for the strengthening of the interaction between the hydrogen-bonding partners on formation of the intermediate. Concomitantly, a hydrogen bond between the enzyme and the substrate may strengthen as a result of conformational changes in the enzyme−intermediate complex, contributing to increased enzyme−intermediate complementarity. Indeed, enhanced interactions between enzymes and intermediates or altered substrates in the transition state are a common theme in catalysis, even for binding determinants on the ligand that appear to be remote from the site of chemistry (*64, 79, 84−86*).

CONCLUSIONS

We have identified α-hydroxybenzylphosphonate and benzohydroxamate as potent reversible competitive inhibitors of mandelate racemase. These analogues share geometric and electronic features with the putative *aci*-carboxylate intermediate and represent the most potent reversible inhibitors of this enzyme reported to date. Comparison of the observed inhibition constants for both carboxylate- and phosphonate-containing analogues indicate that a hydroxyl function located on a ligand's α-carbon is essential for potent inhibition. This observation, combined with the observation that the α-hydroxyl function is required for 1,1-proton transfer (*41*), suggests that the α-hydroxyl function plays a significant role in stabilizing the altered substrate in the transition state. Indeed, removal of the hydrogen bonding interaction between the α-hydroxy function and the carboxamide of Asn 197, as in the N197A mutant, causes a marked reduction in k_{cat}/K_m and binding of intermediate analogues. In addition to providing electrophilic stabilization to the α-carbon via coordination of the active site magnesium, the α-hydroxyl function also promotes catalysis through hydrogen bonding to the side chain of Asn 197.

ACKNOWLEDGMENT

REFERENCES

1. Hegeman, G. D. (1970) *Methods Enzymol. 17*, 670−674.
2. Kenyon, G. L., and Hegeman, G. D. (1979) *Adv. Enzymol. 50*, 325−360.
3. Kenyon, G. L., Gerlt, J. A., Petsko, G. A., and Kozarich, J. W. (1995) *Acc. Chem. Res. 28*, 178−186.
4. Whitman, C. P., Hegeman, G. D., Cleland, W. W., and Kenyon, G. L. (1985) *Biochemistry 24*, 3936−3942.
5. Powers, V. M., Koo, C. W., Kenyon, G. L., Gerlt, J. A., and Kozarich, J. W. (1991) *Biochemistry 30*, 9255−9263.
6. Neidhart, D. J., Howell, P. L., Petsko, G. A., Powers, V. M., Rongshi, L., Kenyon, G. L., and Gerlt, J. A. (1991) *Biochemistry 30*, 9264−9273.
7. Landro, J. A., Kallarakal, A. T., Ransom, S. C., Gerlt, J. A., Kozarich, J. W., Neidhart, D. J., and Kenyon, G. L. (1991) *Biochemistry 30*, 9274−9281.
8. Mitra, B., Kallarakal, A. T., Kozarich, J. W., Gerlt, J. A., Clifton, J. G., Petsko, G. A., and Kenyon, G. L. (1995) *Biochemistry 34*, 2777−2787.
9. Gerlt, J. A., Kenyon, G. L., Kozarich, J. W., Neidhart, D. J., Petsko, G. A., and Powers, V. M. (1992) *Curr. Opin. Struct. Biol. 2*, 736−742.
10. Babbitt, P. C., Hasson, M. S., Wedekind, J. E., Palmer, D. R. J., Barrett, W. C., Reed, G. H., Rayment, I., Ringe, D., Kenyon, G. L., and Gerlt, J. A. (1996) *Biochemistry 35*, 16489−16501.
11. Babbitt, P. C., and Gerlt, J. A. (1997) *J. Biol. Chem. 272*, 30591−30594.
12. Gerlt, J. A. (1998) in *Bioorganic Chemistry: Peptides and Proteins* (Hecht, S. M., Ed.) pp 279−311, Oxford University Press, New York.
13. Eigen, M. (1964) *Angew. Chem., Int. Ed. Engl. 3*, 1−72.
14. Albery, W. J. (1982) *J. Chem. Soc., Faraday Trans. 78*, 1579−1590.
15. Chiang, Y., Kresge, A. J., Santaballa, J. A., and Wirz, J. (1988) *J. Am. Chem. Soc. 110*, 5506−5510.
16. Chiang, Y., Kresge, A. J., Pruszynski, P., Schepp, N. P., and Wirz, J. (1990) *Angew. Chem., Int. Ed. Engl. 29*, 792−794.
17. Amyes, T. L., and Richard, J. P. (1996) *J. Am. Chem. Soc. 118*, 3129−3141.
18. Gerlt, J. A., Kozarich, J. W., Kenyon, G. L., and Gassman, P. G. (1991) *J. Am. Chem. Soc. 113*, 9667−9669.
19. Gerlt, J. A., and Gassman, P. G. (1992) *J. Am. Chem. Soc. 114*, 5928−5934.
20. Gerlt, J. A., and Gassman, P. G. (1993) *J. Am. Chem. Soc. 115*, 11552−11568.
21. Gerlt, J. A., and Gassman, P. G. (1993) *Biochemistry 32*, 11943−11952.
22. Guthrie, J. P., and Kluger, R. (1993) *J. Am. Chem. Soc. 115*, 11569−11572.
23. Bearne, S. L., and Wolfenden, R. (1997) *Biochemistry 36*, 1646−1656.
24. Lolis, E., and Petsko, G. A. (1990) *Annu. Rev. Biochem. 59*, 597−630.
25. Wolfenden, R. (1972) *Acc. Chem. Res. 5*, 10−18.
26. Wolfenden, R. (1974) *Mol. Cell. Biochem. 3*, 207−111.
27. Wolfenden, R. (1976) *Annu. Rev. Biophys. Bioeng. 5*, 271−306.
28. Wolfenden, R., and Frick, L. (1987) in *Enzyme Mechanisms* (Page, M. I., and Williams, J., Eds.) pp 97−122, Royal Society of Chemistry, London.
29. Radzicka, A., and Wolfenden, R. (1995) *Methods. Enzymol. 249*, 284−312.
30. Mader, M. M., and Bartlett, P. A. (1997) *Chem. Rev. 97*, 1281−1301.
31. Porter, D. J. T., and Bright, H. J. (1980) *J. Biol. Chem. 255*, 4772−4780.
32. Flint, D. H. (1994) *Arch. Biochem. Biophys. 311*, 509−516.
33. Schloss, J. V., Porter, D. J. T., Bright, H. J., and Cleland, W. W. (1980) *Biochemistry 19*, 2358−2362.
34. Schloss, J. V., and Cleland, W. W. (1982) *Biochemistry 21*, 4420−4427.
35. Anderson, V. E., Weiss, P. M., and Cleland, W. W. (1984) *Biochemistry 23*, 2779−2786.
36. Wedekind, J. E., Poyner, R. R., Reed, G. H., and Rayment, I. (1994) *Biochemistry 33*, 9333−9342.
37. Genet, R., and Lederer, F. (1990) *Biochem. J. 266*, 301−304.
38. Porter, D. J. T., Rudie, N. G., and Bright, H. J. (1983) *Arch. Biochem. Biophys. 225*, 157−163.
39. Raushel, F. M. (1984) *Arch. Biochem. Biophys. 232*, 520−525.
40. Bearne, S. L., and Kluger, R. (1992) *Bioorg. Chem. 20*, 135−147.
41. Landro, J. A., Gerlt, J. A., Kozarich, J. W., Koo, C. W., Shah, V. J., Kenyon, G. L, Neidhart, D. J., Fujita, S., and Petsko, G. A. (1994) *Biochemistry 33*, 635−643.
42. Kallarakal, A. T., Mitra, B., Kozarich, J. W., Gerlt, J. A., Clifton, J. G., Petsko, G. A., and Kenyon, G. L. (1995) *Biochemistry 34*, 2788−2797.

43. Schafer, S. L., Barrett, W. C., Kallarakal, A. T., Mitra, B., Kozarich, J. W., Gerlt, J. A., Clifton, J. G., Petsko, G. A., and Kenyon, G. L. (1996) *Biochemistry 35*, 5662−5669.

44. Novagen (1997) *pET System Manual*, 7th ed., TB055, pp 18−64.

45. Sambrook, J., Fritsch, E. F., and Maniatis, T. (1989) *Molecular Cloning: A Laboratory Manual*, Cold Spring Harbor Laboratory Press, Plainview, NY.

46. Abramov, V. S. (1950) *Doklady Akad. Nauk. S.S.S.R. 73*, 487−489; *Chem. Abs.* (1951) *45*, 2855*h*.

47. Freeman, S., Irwin, W. J., and Schwalbe, C. H. (1991) *J. Chem. Soc., Perkin Trans. 2*, 263−267.

48. Hoffmann, M. (1985) *Pol. J. Chem. 59*, 395−404.

49. Hoffmann, M. (1988) *Synthesis*, 62−64.

50. Smaardijk, Ab. A., Noorda, S., Bolhuis, F., and Wynberg, H. (1985) *Tetrahedron Lett. 26*, 493−496.

51. Kluger, R., and Chin, J. (1978) *J. Am. Chem. Soc. 100*, 7382−7388.

52. Sekine, M., Futatsugi, T., Yamada, K., and Hata, T. (1982) *J. Chem. Soc., Perkin Trans. 1*, 2509−2513.

53. Fee, J. A., Hegeman, G. D., and Kenyon, G. L. (1974a) *Biochemistry 13*, 2528- 2532.

54. Bearne, S. L., St. Maurice, M., and Vaughan, M. D. (1999) *Anal. Biochem. 269*, 332−336.

55. Sharp, T. R., Hegeman, G. D., and Kenyon, G. L. (1979) *Anal. Biochem. 94*, 329- 334.

56. Kenyon, G. L., and Hegeman, G. D. (1970) *Biochemistry 9*, 4029−4036.

57. Kenyon, G. L., and Hegeman, G. D. (1970) *Biochemistry 9*, 4036−4043.

58. Kresge, A. J. (1991) *Pure Appl. Chem. 63*, 213−221.

59. Chiang, Y., Kresge, A. J., Popik, V. V., and Schepp, N. P. (1997) *J. Am. Chem. Soc. 119*, 10203−10212.

60. Hammond, G. S. (1955) *J. Am. Chem. Soc. 77*, 334−338.

61. Fee, J. A., Hegeman, G. D., and Kenyon, G. L. (1974) *Biochemistry 13*, 2533−2538.

62. Kubala, G., and Martell, A. E. (1982) *Inorg. Chem. 21*, 3007−3013.

63. Tipton, K. F., and Dixon, H. B. F. (1979) *Methods Enzymol. 63*, 183−234.

64. Fersht, A. R. (1999) *Structure and Mechanism in Protein Science*, pp 169−182, 329−331, and 428−438, Freeman, New York.

65. Martin, D. J., and Griffin, C. E. (1965) *J. Org. Chem. 30*, 4034−4038.

66. Kluger, R., Nakaoka, K., and Tsui, W.-C. (1978) *J. Am. Chem. Soc. 100*, 7388−7391.

67. Gulick, A. M., Hubbard, B. K., Gerlt, J. A., and Rayment, I. (2000) *Biochemistry 39*, 4590−4602.

68. Exner, O., Hrdal, M., and Mollin, J. (1993) *Collect. Czech. Chem. Commun. 58*, 1109−1121.

69. Ventura, O. N., Rama, J. B., Turi, L., and Dannenberg, J. J. (1993) *J. Am. Chem. Soc. 115*, 5754−5761.

70. Bagno, A., Comuzzi, C., and Scorrano, G. (1994) *J. Am. Chem. Soc. 116*, 916- 924.

71. Schramm, V. L. (1998) *Annu. Rev. Biochem. 67*, 693−720.

72. Warshel, A. (1991) *Computer Modeling of Chemical Reactions in Enzyme and Solutions*, John Wiley & Sons, New York.

73. Horenstein, B. A., Parkin, D. W., Estupinán, B., and Schramm, V. L. (1991) *Biochemistry 30*, 10788−10795.

74. Horenstein, B. A., and Schramm, V. L. (1993) *Biochemistry 32*, 7089−7097.

75. Horenstein, B. A., and Schramm, V. L. (1993) *Biochemistry 32*, 9917−9925.

76. Wilkinson, A. J., Fersht, A. R., Blow, D. M., and Winter, G. (1983) *Biochemistry 22*, 3581−3586.

77. Wilkinson, A. J., Fersht, A. R., Blow, D. M., Carter, P., and Winter, G. (1984) *Nature 307*, 187−188.

78. Street, I. P., Armstrong, C. R., and Withers, S. G. (1986) *Biochemistry 25*, 6021−6027.

79. Roth, N. J., Rob, B., and Huber, R. E. (1998) *Biochemistry 37*, 10099−10107.

80. Albery, W. J., and Knowles, J. R. (1976) *Biochemistry 15*, 5631−5640.

81. Albery, W. J., and Knowles, J. R. (1977) *Angew. Chem., Int. Ed. Engl. 16*, 285−293.

82. McEwen, W. K. (1936) *J. Am. Chem. Soc. 58*, 1124−1129.

83. Chiang, Y., and Kresge, A. J. (1991) *Science 253*, 395−400.

84. Shan, S., Loh, S., and Herschlag, D. (1996) *Science 272*, 97−101 and references therein.

85. Wolfenden, R. (1999) *Bioorg. Med. Chem. 7*, 647−652.

86. Miller, B. G., Snider, M. J., Short, S. A., and Wolfenden, R. (2000) *Biochemistry 39*, 8113−8118.

87. Sjoberg, P., and Politzer, P. (1990) *J. Phys. Chem. 94*, 3959−3961.

88. Segel, I. H. (1993) *Enzyme Kinetics*, pp 34−37, John Wiley & Sons, New York.